JACS
JOURNAL OF THE AMERICAN CHEMICAL SOCIETY
Article
pubs.acs.org/JACS

Exciplex Formation in Bimolecular Photoinduced Electron-Transfer Investigated by Ultrafast Time-Resolved Infrared Spectroscopy

Marius Koch, Romain Letrun, and Eric Vauthey*

Department of Physical Chemistry, University of Geneva, 30 Quai Ernest-Ansermet, CH-1211 Geneva 4, Switzerland

Supporting Information

ABSTRACT: The dynamics of bimolecular photoinduced electron-transfer reactions has been investigated with three donor/acceptor (D/A) pairs in tetrahydrofuran (THF) and acetonitrile (ACN) using a combination of ultrafast spectroscopic techniques, including time-resolved infrared absorption. For the D/A pairs with the highest driving force of electron transfer, all transient spectroscopic features can be unambiguously assigned to the excited reactant and the ionic products. For the pair with the lowest driving force, three additional transient infrared bands, more intense in THF than in ACN, with a time dependence that differs from those of the other bands are observed. From their frequency and solvent dependence, these bands can be assigned to an exciplex. Moreover, polarization-resolved measurements point to a relatively well-defined mutual orientation of the constituents and to a slower reorientational time compared to those of the individual reactants. Thanks to the minimal overlap of the infrared signature of all transient species in THF, a detailed reaction scheme including the relevant kinetic and thermodynamic parameters could be deduced for this pair. This analysis reveals that the formation and recombination of the ion pair occur almost exclusively via the exciplex.

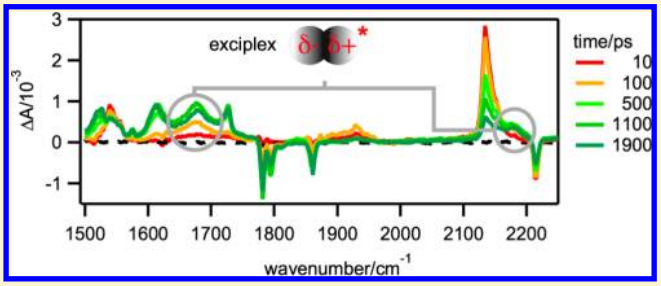

INTRODUCTION

Since the availability of ultrashort pulses in many regions of the electromagnetic spectrum, the dynamics of photochemical processes can be monitored with an unprecedented precision. Among these processes, photoinduced electron-transfer reactions are most probably the most investigated.[1−12] A large variety of species, namely exciplexes, tight/contact, loose/solvent-separated ion pairs (TIP/CIP and LIP/SSIP) have been suggested as possible intermediates in bimolecular photoinduced charge separation (CS) reactions, depending on the environment and driving force (Figure 1).[13−18]

So far, most of the ultrafast spectroscopic investigations on bimolecular photoinduced CS have been performed using transient electronic absorption spectroscopy. Whereas very powerful to distinguish molecules in different electronic states, this technique does not allow the above-mentioned intermediates to be properly differentiated. On the other hand, transient vibrational spectroscopy has proven to enable distinction between ion pairs and free ions as well as between TIPs and LIPs.[19,20] This strength arises from the relatively large number of bands observable in a transient vibrational spectrum, the narrow width of these bands, and the high sensitivity of the vibrational frequencies to changes of the electronic distribution in the molecule.[21] For example, the C≡N stretching frequencies in TIPs and LIPs, formed upon CS between perylene in the S_1 state and tetracyanoethylene, were found to differ by 5 cm^{-1}.[20] Another recent study on adenine-thymine heterodimers further illustrates the strength of transient IR absorption spectroscopy to detect charge-transfer excited states.[22]

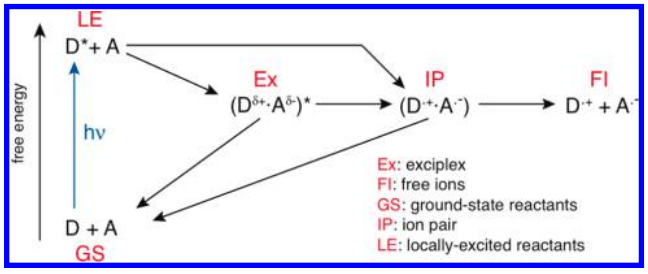

Figure 1. Simplified electronic energy level scheme for a bimolecular photoinduced CS in polar solvents (possible equilibria have been omitted).

To the best of our knowledge, exciplexes, which are omnipresent in photochemistry, have not been studied so far using transient IR absorption spectroscopy. Exciplexes appear as intermediates in intra-[23−26] and intermolecular photoinduced CS in solution,[27−31] in organic semiconductors for photovoltaics[32−38] or light emitting diodes (OLEDs),[39−44] in DNA,[22,45−47] in photosynthetic reaction centers,[48] and in various organic photochemical reactions.[49−51] Theoretically, exciplexes can be described by a linear combination of locally excited (LE) reactants and ion pair (IP) wave functions with weighting coefficients that depend on the redox properties of

Received: January 24, 2014
Published: February 14, 2014

dx.doi.org/10.1021/ja500812u | J. Am. Chem. Soc. 2014, 136, 4066−4074

the constituents and the polarity of the environment. They are the predominant product of electron-transfer fluorescence quenching in non-polar media, liquids as well as polymers.[27,52,53] As such, they can be considered as the product of an incomplete CS. In highly polar media, they have only been reported with weak donor/acceptor (D/A) pairs, i.e., for which the CS driving force, $-\Delta G_{CS}$, is below ca. 0.5 eV.[28,54,55] In such polar environments, quenching generally results in the direct formation of ion pairs, TIPs and/or LIPs (Figure 1). In medium polarity media, exciplexes coexist with ion pairs. However, their exact role, i.e., intermediates on the way to the ion pairs or parallel quenching product, has been highly debated[13,56,57] and is still being investigated. Such knowledge is crucial not only for our understanding of bimolecular photoinduced processes but also for potential applications such as organic solid-state photovoltaic devices, where the photoinduced CS occurs in a weakly polar environment and the diffusion of the excited reactants and the ionic product is replaced by the hopping of the excitation energy and the electric charges.[58−63]

Exciplexes have been mostly identified by their emission, which is, in the most favorable cases, spectrally well separated from the LE fluorescence.[14,52,64] However, as this transition is characterized by a substantial charge-transfer character, its oscillator strength is generally much smaller than that of the LE emission, making its observation by ultrafast fluorescence techniques very challenging. Moreover, in many cases, the exciplex and LE fluorescence bands overlap, and therefore the extraction of species-associated data is difficult and often indirect. The combination of emission and magnetic field, which has been shown to be very powerful for the understanding of the role of exciplexes, suffers from similar problems.[65,66]

The involvement of exciplexes has also been inferred from transient electronic absorption spectroscopy experiments. In those cases however, the spectral features of the exciplex were very similar to those of the ions or charge-separated state, and the assignment of the transient to an exciplex was mostly based on other considerations such as its dynamics, the nature of the environment, or the detection of a characteristic emission.[26,67−69]

We present here our investigation, using transient IR absorption spectroscopy, of the dynamics of bimolecular photoinduced CS reaction with three D/A pairs, characterized by a small ΔG_{CS}, in a highly polar solvent, acetonitrile (ACN), and a medium polar solvent, tetrahydrofuran (THF) (Chart 1). Vibrational bands in the mid-IR that are distinct by their frequency and time evolution from those of the LE and IP states are observed and assigned to an exciplex. A detailed analysis of the transient IR absorption spectra reveals that in THF, this exciplex is not a quenching side product but a key intermediate for the formation and decay of the ion pair. Additionally, original structural information on the exciplex deduced from polarization-resolved measurements is described.

Chart 1. Electron Donors (Chromophores), Acceptor, and Solvents[a]

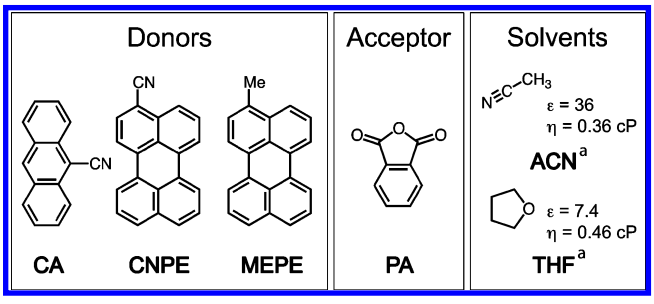

[a]Ref 70; ε: relative permittivity; η: viscosity.

RESULTS AND DISCUSSION

The D/A pairs selected for this investigation consist of the weak electron donors 9-cyanoanthracene (CA), 3-cyanoperylene (CNPE), or 3-methylperylene (MEPE) that also act as chromophores and of phthalic anhydride (PA) as acceptor (Chart 1). These pairs allow a variation of the CS driving force, $-\Delta G_{CS}$, from weak to moderate (Table 1) and have good IR marker modes, such as the C≡N, C═O, and C═C stretching vibrations, on both D and A.

Table 1. Energetic Parameters for CS between the Excited Donor, D*, and PA

D	E_{00}[a] (eV)	E_{ox}[b] (V)	τ_f (ns)	ΔG_{CS}(ACN)[c] (eV)	ΔG_{CS}(THF)[c] (eV)
CA	2.96[d]	1.57[e]	11.4	−0.13	0.08
CNPE	2.65[f]	1.21[f]	5.1	−0.18	0.03
MEPE	2.83[f]	1.00[f]	4.2	−0.57	−0.36

[a]S_1 state energy. [b]vs SCE. [c]Calculated from eq (16) in ref 71 with E_{red}(PA) = −1.31 V vs SCE,[72] ionic radii of 3.5 Å, and contact distance. [d]Ref 73. [e]Ref 74. [f]Ref 75.

Fluorescence. Addition of PA to solutions of the donors in ACN and THF leads to a substantial decrease of the fluorescence intensity. For CA and CNPE in THF, this effect is accompanied by a small change in the emission band shape, that is due to an exciplex, whose emission spectrum overlaps with that of the LE fluorescence. Polynomial analysis of the emission band shape with and without PA allowed extracting the exciplex spectra shown in Figure 2. The overlap of the exciplex and LE emission agrees with the weak CS driving force (Table 1).

The quenching rate constants have been determined from a Stern−Volmer analysis of the decrease of the stationary fluorescence intensity upon addition of PA (Figure S1). For CA and CNPE, quenching by PA in THF is about 10 times slower than diffusion, while it is of the same order of magnitude in ACN. For MEPE, quenching is diffusion limited in both solvents (Table S1). Consequently, the quenching dynamics of CA and CNPE in THF can be expected to be exponential and mostly devoid of the complications arising from the static and the transient effects,[76−78] as also supported by the linearity of their Stern−Volmer plots. Despite this, the fluorescence decays of CA and CNPE are only exponential at quencher concentrations below ca. 0.1 M. Above this value, they can be reproduced with the sum of two exponential functions with a main decay component that becomes faster with increasing PA concentration and a weaker one of the order of 1 ns with a relative amplitude that increases with PA concentration (Figure S2). As will be shown below, this behavior arises from an equilibrium between the LE reactants and the exciplex. However, as evidenced below, the overall reaction scheme is too complex for these fluorescence decays to be analyzed with the Birks' excimer model,[79] as usually done.[80] The fluorescence decay of MEPE accelerates with increasing PA concentration as

dx.doi.org/10.1021/ja500812u | J. Am. Chem. Soc. 2014, 136, 4066−4074

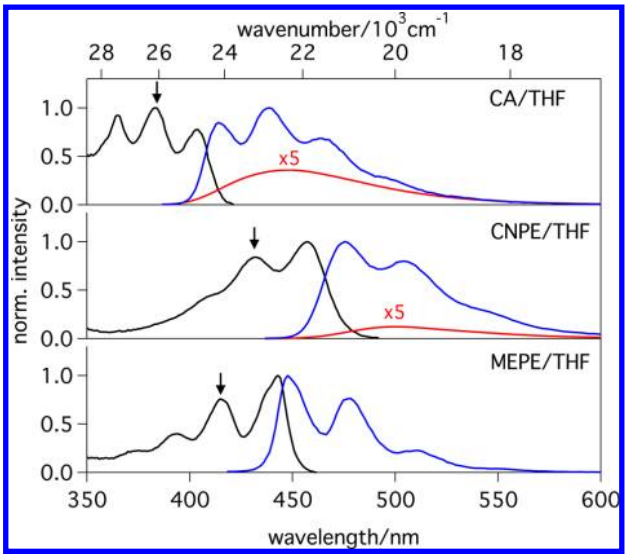

Figure 2. Absorption (black) and emission (blue) spectra of the three donors in THF and of the exciplex (red) measured in the presence of 0.1 M PA. The black arrows indicate the excitation wavelength.

well. However, fast decay components appear above 0.02 M PA. They can be ascribed to the static and transient stages of the quenching, in agreement with the departure from linearity of the Stern−Volmer plots.

Transient Electronic Absorption. Transient absorption measurements were first performed in the visible region, selected transient spectra in THF being shown in Figures 3 and S3. The quenching of CA* results in a decrease of the positive band at 565 nm due to a $S_n \leftarrow S_1$ transition and of the negative band in the 440−480 nm region arising from $S_1 \rightarrow S_0$ stimulated emission. The quenching product can only be guessed in THF but is clearly visible in ACN (Figure S4), with a band at ca. 440 nm that can be ascribed to the radical cation of the donor, $CA^{\bullet+}$. The radical cation bands can be better seen with both $CNPE^{\bullet+}$ and $MEPE^{\bullet+}$ at 550 nm (Figure S3). The radical anion $PA^{\bullet-}$ cannot be observed because its absorption band in the 410−420 nm region is hidden by the bleach of the $S_1 \leftarrow S_0$ absorption.[81] None of the transient electronic absorption spectra measured here exhibits any feature that could be ascribed to an exciplex.

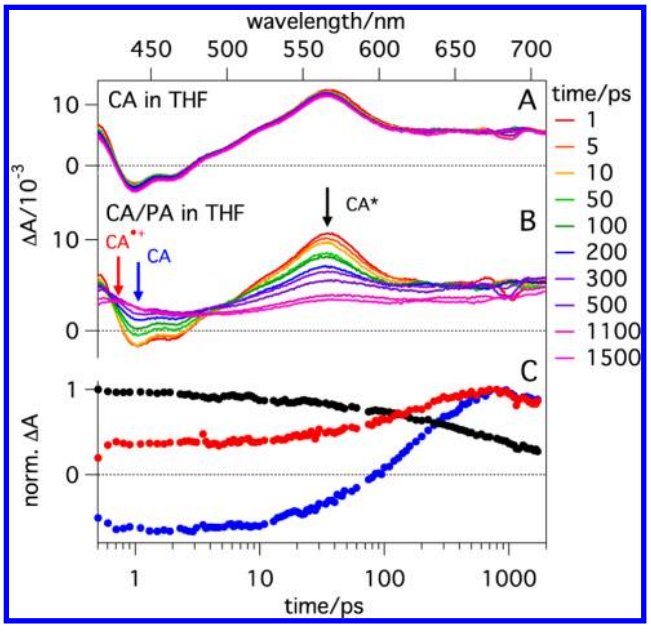

Figure 3. Transient electronic absorption spectra measured in THF at various time delays after 400 nm excitation of CA alone (A) and in the presence of 1 M PA (B). The arrows indicate the wavelengths selected for the time profiles shown in (C).

Transient Vibrational Absorption. Transient absorption experiments were then performed in the mid-IR region, some of the spectra obtained with CA/PA in THF in the 1500−1750 cm^{-1} window being shown in Figure 4A. The transient spectra

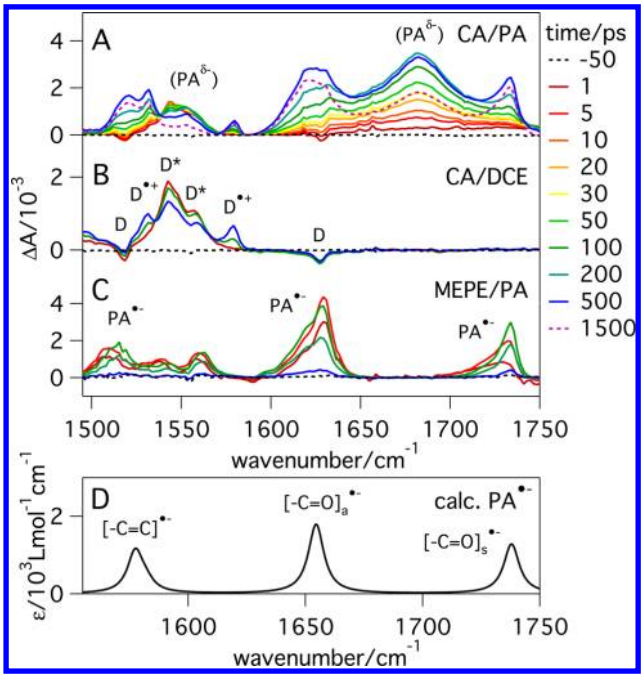

Figure 4. Transient IR spectra measured in THF at different time delays after 400 nm excitation of CA with 1 M PA (A) and 1 M DCE (B) and of MEPE with 1 M PA (C). (D) Calculated IR absorption spectrum of $PA^{\bullet-}$.

are initially dominated by two bands around 1540−1550 cm^{-1}, whose decay is accompanied by the rise of six new bands, that reach a maximum intensity at about 500 ps before starting to decrease on a longer time scale. To assign these transient bands to a given species/state and vibrational mode, the same measurements were performed with dicyanoethylene (DCE) as quencher instead of PA. Neither DCE nor $DCE^{\bullet-}$ have vibrational modes in this frequency region,[75] allowing the identification from the spectra at short time delays of [−C═C]* ring vibrations of CA* at 1543 and 1557 cm^{-1} (Figure 4B). These bands decrease with time as quenching takes place and two news band at 1532 and 1579 cm^{-1} rise, which can be ascribed to $[-C{=}C]^{\bullet+}$ ring vibrations of $CA^{\bullet+}$. Additionally, the two negative ground-state bleach features at 1519 and 1627 cm^{-1} can be assigned to [−C═C] ring vibrations of CA. Similar measurements with MEPE instead of CA allowed identification of $PA^{\bullet-}$ bands at ca. 1520, 1620, and 1735 cm^{-1} (Figure 4C). These frequencies coincide very well with those obtained from DFT calculations using the B3LYP functional and 6-31G(d) basis set, without any scaling factor (Figure 4D). The 1520 cm^{-1} band can thus be assigned to a $[-C{=}C]^{\bullet-}$ aromatic ring vibration, whereas those at 1620 and 1735 cm^{-1} can be interpreted as the antisymmetric and

dx.doi.org/10.1021/ja500812u | J. Am. Chem. Soc. 2014, 136, 4066−4074

symmetric $[-C{=}O]^{\bullet-}$ stretching vibrations of $PA^{\bullet-}$, respectively. Calculations for the neutral PA predict the frequencies of these modes to be above 1760 cm^{-1} (Figure S5). These large frequency down shifts upon reduction of PA illustrate the high sensitivity of the vibrational frequencies to variations of electronic density.

Two bands in the transient spectrum measured with CA/PA, a prominent one around 1682 cm^{-1} and a weak one at ~1552 cm^{-1}, still remain to be interpreted. We assign them to the exciplex, $(CA^{\delta+}/PA^{\delta-})^*$, whose presence was already concluded from the fluorescence. Because CS is incomplete in an exciplex, the vibration frequencies can be expected to lie between those of the neutral ground-state reactants, CA/PA, and those of the ions, $CA^{\bullet+}/PA^{\bullet-}$. Therefore the 1552 and 1682 cm^{-1} bands can be ascribed to the $[-C{=}C]^{\delta-}$ and $[-C{=}O]^{\delta-}$ stretching modes of $PA^{\delta-}$, respectively. The second $[-C{=}O]^{\delta-}$ stretching band that should be located above 1735 cm^{-1} cannot be observed because the probe IR light between 1760 and 1865 cm^{-1} is totally absorbed by the quencher present at high concentration.

The assignment to an exciplex is strengthened by the dependence of these bands on the solvent polarity. The $[-C{=}O]^{\delta-}$ band is indeed still visible but substantially weaker in ACN (Figure 5A,B). A similar decrease in intensity is observed with CNPE (Figure 5 C,D). The dependence of the intensity of these IR bands on the donor is similar to that observed with the exciplex fluorescence (Figure 2): The intensity is the strongest with CA, substantially weaker with CNPE, and below the limit of detection with MEPE (Figure 5 E,F). This trend also correlates with the CS driving force (Table 1): A larger driving force can favor direct formation of ion pairs upon quenching, but it also results in an exciplex with a larger charge-transfer character. In this case, the oscillator strength for emission is smaller and the vibrational bands closer to those of the ions. Of course other factors such as the electronic structure can also contribute to this donor dependence of the band intensity.

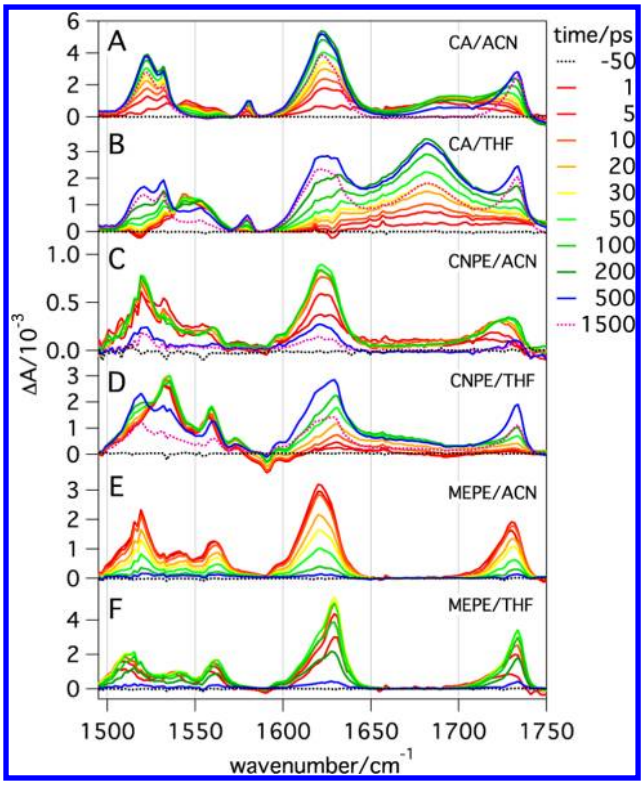

Figure 5. Transient IR spectra measured at different time delays after 400 nm excitation of CA, CNPE, and MEPE in ACN and THF in presence of 1 M PA.

A further confirmation of the origin of these bands is obtained from the transient absorption spectra measured with both CA and CNPE in the C≡N stretching region (Figures 6 and S7). The spectra with CA/PA in ACN exhibit a positive band at 2129 cm^{-1} due to the C≡N stretching of CA*, $[-C{\equiv}N]^*$, which decays as quenching takes place, and a negative band at 2211 cm^{-1} arising from the bleach of the C≡N absorption of CA in the ground state, $[-C{\equiv}N]$, and whose intensity remains constant within the time window of the experiment. No cation band can be observed, in agreement with the very small oscillator strength of the $[-C{\equiv}N]^{\bullet+}$ stretching mode obtained from the quantum chemical calculations (Figure S6).

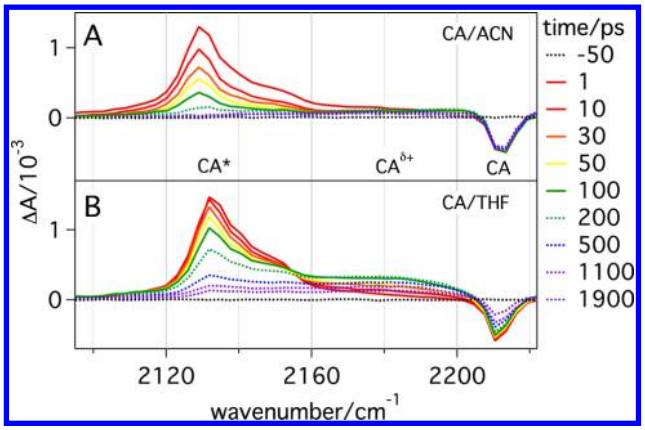

Figure 6. Transient IR spectra measured at several time delays after 400 nm excitation of CA with 1 M PA in ACN (A) and THF (B).

In THF, the early spectra resemble those in ACN, but the decay of the $[\text{-}C{\equiv}N]^*$ band is accompanied by the appearance of a broad band in the 2160−2200 cm^{-1} region. After ca. 300 ps, its intensity decreases slightly but less than that of the $[\text{-}C{\equiv}N]^*$ band. Such band is also present but hardly visible with CNPE in THF (Figure S7). It is ascribed to the exciplex and originates from its other constituent, namely from $CA^{\delta+}$ and $CNPE^{\delta+}$. The oscillator strength of the $[-C{\equiv}N]^{\delta+}$ stretching mode is smaller than that of $[\text{-}C{\equiv}N]^*$ but, because of the partial charge separation, still large enough compared to that of $[-C{\equiv}N]^{\bullet+}$ to make its absorption visible.

The same measurements were repeated with 0.2 M PA instead of 1 M, and the resulting spectra are basically identical (Figure S8), although their time evolution is slower, as expected.

Apart from these exciplex bands, Figure 5 also reveals that the shape and position of the $PA^{\bullet-}$ bands depend somewhat on donor and solvent. For example, the width of the $[-C{=}O]^{\bullet-}$ stretching band at 1620 cm^{-1} changes with time, especially with CNPE and MEPE in THF (Figure 5D,F). We suggest that this is due to the presence of ion pairs with different mutual orientations/distances such as tight (TIPs) and loose ion pairs (LIPs).[20,82] The electronic density on $PA^{\bullet-}$, thus the vibrational frequency, depends on the electronic coupling between the ionic constituents. TIPs are predominantly formed at early time

dx.doi.org/10.1021/ja500812u | J. Am. Chem. Soc. 2014, 136, 4066−4074

through static quenching, whereas LIPs are generated later via diffusion.[83] This time dependence is less pronounced in ACN, most probably because of the higher solvent polarity. These relatively small effects will not be discussed further here but will be addressed elsewhere; the main scope of the present report being the exciplex bands.

The exciplex bands, best seen with $(CA^{\delta+}/PA^{\delta-})^*$ in THF, are substantially broader than those of the ions. This most probably arises from fluctuations, during the lifetime of the exciplex, of the distance or the mutual orientation of the constituents, hence of the electronic coupling and the vibrational frequency. As will be shown below, the lifetime of the exciplex is substantially longer than the time scale of reorientational motion. If the geometry of the exciplex remained constant during its lifetime, a distribution of geometries would lead to an inhomogeneous broadening of the band. In such case, one could expect to observe changes in the band shape with time, as it would be very improbable that exciplexes with different geometry have exactly the same lifetime. As this is not the case, a fluctuation of the mutual orientation can be assumed, in agreement with the polarization anisotropy measurements described below.

Kinetics and Reaction Scheme. We now concentrate on the time evolution of the transient IR spectra, in particular those measured with the CA/PA pair in THF, where the exciplex band is the most prominent (Figures 5B and 6B). Time profiles of the transient absorption at the frequencies of CA, CA*, $PA^{\bullet-}$, and $PA^{\delta-}$ bands are illustrated in Figure 7. The

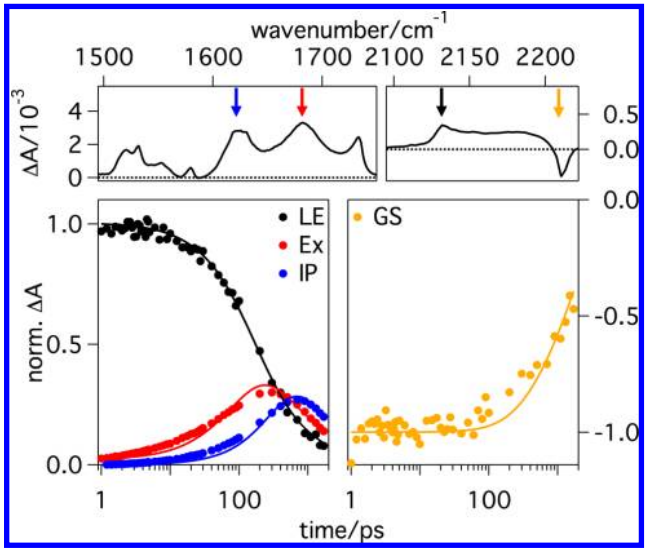

Figure 7. Time profiles of the transient absorption measured with CA and 1 M PA in THF at the frequencies indicated by the arrows in the spectra at the top (measured at 500 ps) and reflecting the temporal evolution of the CA ground (GS) and excited states (LE), ions (IP) and exciplex (Ex) populations. The solid lines are the best fits from a global target analysis.

transient absorption profile at the frequency of a $CA^{\bullet+}$ band is identical to that of $PA^{\bullet-}$, as expected, and is thus not shown. The following observations can be done: (1) the decay of the CA* band is biphasic with the slow component similar to the decay of the exciplex and ion bands; (2) the rise of the exciplex band is substantially faster than that of the ion band; and (3) the ground-state recovery occurs on a similar time scale as the decay of the exciplex and ions bands.

Observation 1 points to the existence of an equilibrium between the LE reactants and the exciplex and/or the ion pair populations, as already anticipated from the time-resolved fluorescence results. From 2, one can conclude that exciplex and ion pair are not exclusively formed directly from the LE reactants via two competing quenching processes. If this were the case, the rise times of both bands should be identical. Finally, 3 indicates that neither the exciplex nor the ion pair dissociate into free ions, which are long-lived. As a comparison, in ACN, the ground-state population does not recover within the time window of the experiment (Figure 6A), indicating that most ion pairs dissociate into free ions, that eventually recombine on the microsecond time scale.[84]

More quantitative information was obtained from a global target analysis of these time profiles (see Supporting Information for details). The most simple reaction scheme able to satisfactorily reproduce the experimental data is shown in Scheme 1, together with the time constants. It appears that

Scheme 1. Target Model Used to Reproduce the Kinetics Measured Experimentally with CA and 1 M PA in THF[a]

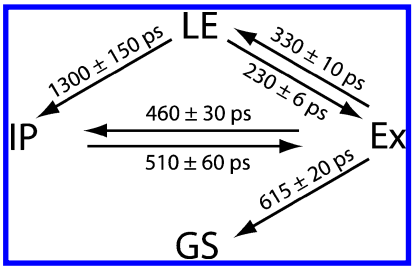

[a]LE is the locally excited state, Ex the exciplex, IP the ion pair state, and GS the ground state.

most of the ion pair population is generated reversibly from the exciplex, which is itself in equilibrium with the LE reactants population. Moreover, the ground-state population recovers through the decay of the exciplex only. The agreement between the calculated and measured time profiles is not perfect as shown in Figure 7, but can be considered as very good in view of the relative crudeness of the model. The strongest discrepancy, that can be observed in the rise of the exciplex and ion pair populations, can most probably be accounted for by the assumption that the static and transient stages of the quenching can be totally neglected. Whereas this is probably true at low quencher concentrations, this assumption may no longer fully holds at 1 M PA. However, differential encounter theory, which has been successfully used to account for such non-Markovian effects,[85,86] cannot be applied to describe reversible processes as it is the case here. Introducing non-Markovian effects in the reaction Scheme 1 would require integral encounter theory,[87] which is far beyond the scope of this investigation.

Further confirmation of the validity of this scheme was obtained by repeating the global analysis with the entire transient spectra in the 1500−1750 cm^{-1} and 2100−2220 cm^{-1} windows using the time constants shown in Scheme 1 as fixed parameters, in order to obtain the difference absorption spectra of each individual species. The resulting species-associated difference spectra (SADS) are shown in Figure 8. The SADS found for the LE reactants and the ions are in good agreement with the experimental transient spectra (Figures 4B,C and 6). Indeed, the spectrum of the ion pair is perfectly reproduced in

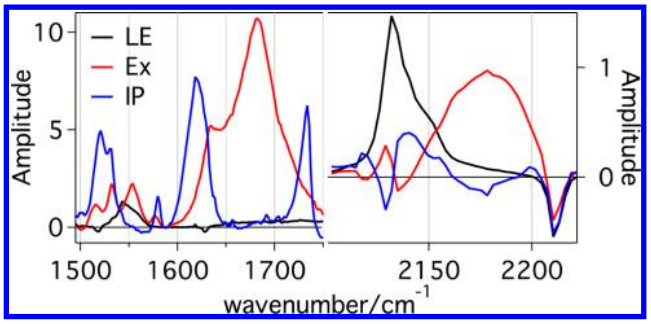

Figure 8. Species-associated difference spectra obtained from a global target analysis of the transient IR spectra measured with CA and 1 M PA in THF using the time constants shown in Scheme 1 as fixed parameters.

the C═C and C═O region. On the other hand, the ion pair SADS suggests that the C≡N stretching band of $CA^{\bullet+}$ is masked by the more intense one of CA*, as already anticipated. The exciplex SADS shows pronounced absorption around 1550, 1680, and 2180 cm^{-1}. The small ion features at 1519, 1532, 1579, and 1630 cm^{-1} are probably artifacts due to the relative crudeness of the model, as discussed above.

It should be noted that fits of similar quality as that shown in Figure 7 could also be obtained with other schemes (Figure S9). However, the resulting time constants yielded SADS combining spectral features belonging to different species, as shown in Figure S9. Therefore, these alternative schemes were discarded.

According to Scheme 1, the equilibrium constant between the LE reactant, CA*/PA, and the exciplex amounts to 1.4, whereas that between the exciplex and the ion pair is slightly below unity, i.e., 0.9. From these equilibrium constants, both the free enthalpy for exciplex formation, ΔG_{EX}, and that for exciplex dissociation into an ion pair, ΔG_{IP}, appear to be very small, i.e., −9 and 3 meV, respectively. The latter value is consistent with those obtained for other exciplexes using time-resolved fluorescence measurements.[88] The free enthalpy for CS, $\Delta G_{CS} = \Delta G_{EX} + \Delta G_{IP}$, is thus close to zero. This agrees very well with the CS driving force in THF estimated from the Weller equation (Table 1). Accordingly, the LE reactants and the ion pair should also be in equilibrium. However, the time constant for the back reaction from the ion pair to the LE reactants is predicted to be too large, i.e., 1.6 ns, for this process to contribute significantly to the dynamics measured in the 0−1.8 ns time window.

Finally, Scheme 1 reveals that the direct charge recombination (CR) of the ions pair is not operative with CA/PA in THF. Because of its large driving force, $-\Delta G_{CR} = E_{00} + \Delta G_{CS} \simeq 2.9$ eV, CR should occur in the deep inverted region and thus be slow.[73,89,90] Moreover, electronic coupling within the ion pair can be expected to be substantially smaller than in the exciplex, and therefore, CR should be substantially slower than the decay of the exciplex. As a consequence, this process is not sufficiently fast to significantly influence the ion pair dynamics.

In ACN, a similar global analysis could not be performed reliably because of the relative weakness of the exciplex bands and their overlap with more intense bands due to other populations. However, the relative intensity of the IR bands points to the ion pair as the dominant quenching product. The absence of ground-state recovery together with the complete decay of the exciplex bands within the time window of the experiment reveal that the exciplex is converted into an ion pair, which itself separates into free ions.

These results are consistent with those from previous investigations based on fluorescence and obtained from an elaborate analysis of the magnetic field effect on the exciplex fluorescence[18,66] or from detailed measurements of the fluorescence lifetime and quantum yield of exciplexes in various solvents.[28,88] In those cases however, the exciplex and LE fluorescence had to be well separated. Moreover, none of these two approaches allows the simultaneous observation of all populations involved in the reaction and the extraction of all relevant time constants, as achieved here.

Mutual Orientation. Further information on the exciplex was obtained from the polarization anisotropy, r, of the transient IR bands:

$$r(t) = \frac{\Delta A_{\parallel}(t) - \Delta A_{\perp}(t)}{\Delta A_{\parallel}(t) + 2\Delta A_{\perp}(t)} \quad (1)$$

where $\Delta A_{\parallel}$ and $\Delta A_{\perp}$ are the transient absorbance measured with the IR probe light polarized parallel and perpendicular, respectively, relative to the polarization of the 400 nm pump light.[91] The initial anisotropy, r_0, before its decay by reorientational motion, depends on the angle β between the probed vibrational transition dipole moment, $\vec{\mu}_{vib}$, and the electronic transition dipole moment associated with the 400 nm excitation, $\vec{\mu}_{el}$ (Figure 9):

$$r_0 = \frac{3\cos^2\beta - 1}{5} \quad (2)$$

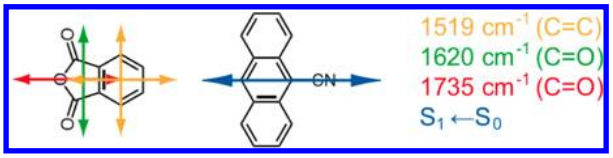

Figure 9. Calculated vibrational transition dipole moments $\vec{\mu}_{vib}$ of $PA^{\bullet-}$ and $S_1 \rightarrow S_0$ transition dipole moment $\vec{\mu}_{el}$ of CA.

As a test, the r_0 values of the C≡N stretching band of CA* and CA in both ACN and THF were found to be close to 0.4 (Figure S10 and Table 2), as expected for parallel $\vec{\mu}_{vib}$ and $\vec{\mu}_{el}$. Similar measurements were performed with the exciplex band ascribed to the antisymmetric C═O stretching of $PA^{\delta-}$, with $\vec{\mu}_{vib}$ oriented perpendicularly to the molecular axis (green arrow in Figure 9). In both solvents, an initial anisotropy of -0.08 ± 0.01 was found (Figure 10), the limits of error being estimated from the results of several measurements. If the mutual orientation of the constituents in the exciplex was unique, eq 2 could be used as such to determine the angle β.[92] However, temporal fluctuations of this angle are expected as discussed above. Assuming a Gaussian distribution of β centered at 90° and a sandwich-like mutual orientation of the exciplex constituents, a r_0 value of −0.08 is obtained with a width of 40°. Of course, other β values cannot be excluded, but some, i.e., a β centered around 0°, can be clearly eliminated. Similarly, a random β with the two constituents in a sandwich-like geometry can also be excluded as it would yield a r_0 value of 0.1. Knowledge of the initial anisotropy of the symmetric C═O stretching of $PA^{\delta-}$ would allow more precise conclusion on the exciplex structure, but, as discussed above, this band cannot be observed.

dx.doi.org/10.1021/ja500812u | J. Am. Chem. Soc. 2014, 136, 4066−4074

Table 2. Parameters Associated with Anisotropy Decay Measured with CA with and without 1M PA in ACN and THF[a]

	CA*		CA		$PA^{\delta-}$	
	r_0	τ_r (ps)	r_0	τ_r (ps)	r_0	τ_r (ps)
ACN	0.34 ± 0.01	9.0 ± 0.2	0.35 ± 0.01	7.6 ± 0.5		
ACN + PA	0.32 ± 0.01	12.0 ± 1	0.41 ± 0.01	12.0 ± 1	−0.08 ± 0.01	25.0 ± 5
THF	0.34 ± 0.01	11.5 ± 0.5	0.38 ± 0.02	10.0 ± 1		
THF + PA	0.31 ± 0.01	15.0 ± 1	0.35 ± 0.01	15.0 ± 2	−0.08 ± 0.01	31.0 ± 7

[a]The limits of error were estimated from several measurements. CA*: measured a 2129 cm^{-1} (ACN) and 2132 cm^{-1} (THF); CA: measured at 2211 cm^{-1}; $PA^{\delta-}$: measured a 1691 cm^{-1} (ACN) and 1682 cm^{-1} (THF).

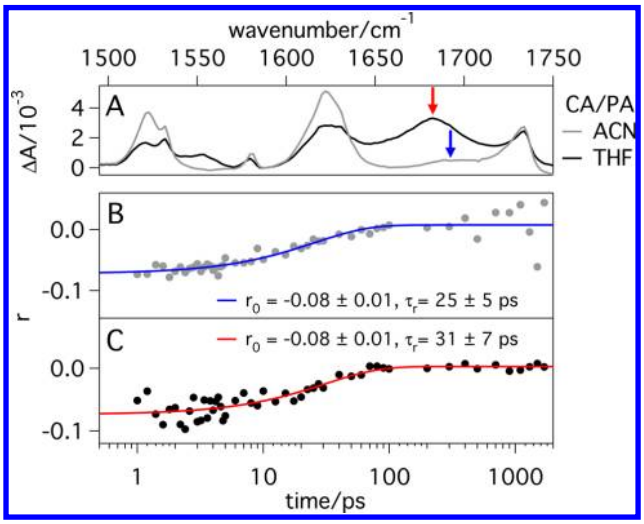

Figure 10. Temporal evolution of the anisotropy measured with CA and 1 M PA in ACN (B) and THF (C) at wavenumbers (1691 cm^{-1} in ACN, 1682 cm^{-1} in THF) corresponding to a $PA^{\delta-}$ exciplex band as indicated by the arrows in the transient spectra (A).

The anisotropy decay time, τ_r, of the exciplex band amounts to 25 ps in ACN and 31 ps in THF and is about three times as long as those measured with CA in both ground and excited states in the absence of PA (Table 2). An increase of the viscosity of the solution due to the presence of quencher cannot account for this effect, as illustrated in Table 2, as a difference of a factor two is still observed upon addition of 1 M PA. The slowing down of the anisotropy decay observed in all cases by going from ACN to THF can be well accounted for by the larger viscosity of THF compared with ACN (Chart 1). The τ_r value measured with the exciplex band reveals that the hydrodynamic volume of the $PA^{\delta-}$ constituent is about twice as large as that of CA. This is possible if the reorientation of $PA^{\delta-}$ involves the concerted motion of the other constituent, $CA^{\delta+}$. Therefore, this longer anisotropy decay time can be assigned to the reorientation of the whole exciplex, whose hydrodynamic volume does not only depend on the molecular volume itself but also on the shape of the exciplex and on its interaction with the solvent. As a consequence, the increase of τ_r by a factor two, by going from CA to the exciplex, can be easily justified.

CONCLUSIONS AND OUTLOOK

This investigation demonstrates the strength of transient IR absorption spectroscopy for investigating the mechanism of bimolecular photoinduced electron-transfer reactions, as it allows intermediates with very similar electronic absorption spectra, such as exciplexes and ion pairs, to be distinguished. In the case of the CA/PA pair, we could thus show that in a medium polarity solvent, like THF, ion pairs are almost exclusively generated upon dissociation of the exciplex and that their recombination also occurs with the exciplex as intermediate. Furthermore, thermodynamic parameters, such as the driving forces for exciplex formation, could be estimated experimentally. The approach presented here is thus much more direct than those based on fluorescence, as it allows simultaneous observation of all species and not only of those exhibiting emission. Our data also evidence the existence of preferential mutual orientations of the donor and acceptor units in the exciplex. Moreover, the two units are sufficiently coupled to have their reorientational motion correlated.

Similar measurements with other donor−acceptor pairs and solvents are required to obtain a more comprehensive understanding of the structure and role of the exciplexes in photoinduced electron-transfer reactions. Extension to two-dimensional IR spectroscopy will yield even deeper insight into the structure of the exciplexes.

ASSOCIATED CONTENT

Supporting Information

Experimental section and procedures, fluorescence quenching, time-resolved fluorescence, transient electronic and infrared absorption spectra, polarization anisotropy. This material is available free of charge via the Internet at http://pubs.acs.org.

AUTHOR INFORMATION

Corresponding Author

eric.vauthey@unige.ch

Notes

The authors declare no competing financial interest.

ACKNOWLEDGMENTS

This work was supported by the Fonds National Suisse de la Recherche Scientifique through project no. 200020-147098 and the NCCR MUST and by the University of Geneva.

REFERENCES

(1) Gould, I. R.; Farid, S. *Acc. Chem. Res.* **1996**, *29*, 522.
(2) Bixon, M.; Jortner, J. *Adv. Chem. Phys.* **1999**, *106*, 35.
(3) Mataga, N.; Miyasaka, H. *Adv. Chem. Phys.* **1999**, *107*, 431.
(4) Guldi, D. M.; Luo, C.; Prato, M.; Troisi, A.; Zerbetto, F.; Scheloske, M.; Dietel, E.; Bauer, W.; Hirsch, A. *J. Am. Chem. Soc.* **2001**, *123*, 9166.
(5) Small, D. W.; Matyushov, D. V.; Voth, G. A. *J. Am. Chem. Soc.* **2003**, *125*, 7470.
(6) Liu, M.; Ito, N.; Maroncelli, M.; Waldeck, D. H.; Oliver, A. M.; Paddon-Row, M. N. *J. Am. Chem. Soc.* **2005**, *127*, 17867.
(7) Vauthey, E. *J. Photochem. Photobiol. A* **2006**, *179*, 1.
(8) Albinsson, B.; Mårtensson, J. *J. Photochem. Photobiol. C* **2008**, *9*, 138.
(9) Gust, D.; Moore, T. A.; Moore, A. L. *Acc. Chem. Res.* **2009**, *42*, 1890.

(10) Bottari, G.; de la Torre, G.; Guldi, D. M.; Torres, T. s. *Chem. Rev.* **2010**, *110*, 6768.
(11) Karlsson, S.; Boixel, J.; Pellegrin, Y.; Blart, E.; Becker, H.-C.; Odobel, F.; Hammarström, L. *Faraday Discuss.* **2012**, *155*, 233.
(12) Rosspeintner, A.; Lang, B.; Vauthey, E. *Annu. Rev. Phys. Chem.* **2013**, *64*, 247.
(13) Weller, A. *Pure Appl. Chem.* **1982**, *54*, 1885.
(14) Gould, I. R.; Young, R. H.; Mueller, L. J.; Albrecht, A. C.; Farid, S. *J. Am. Chem. Soc.* **1994**, *116*, 8188.
(15) Kikuchi, K.; Niwa, T.; Takahashi, Y.; Ikeda, H.; Miyashi, T.; Hoshi, M. *Chem. Phys. Lett.* **1990**, *173*, 421.
(16) Nicolet, O.; Vauthey, E. *J. Phys. Chem. A* **2003**, *107*, 5894.
(17) Kuzmin, M. G.; Soboleva, I. V.; Dolotova, E. V. *J. Phys. Chem. A* **2007**, *111*, 206.
(18) Kattnig, D. R.; Rosspeintner, A.; Grampp, G. *Angew. Chem., Int. Ed.* **2008**, *47*, 960.
(19) Vauthey, E.; Parker, A. W.; Phillips, D.; Nohova, B. *J. Am. Chem. Soc.* **1994**, *116*, 9182.
(20) Mohammed, O. F.; Adamczyk, K.; Banerji, N.; Dreyer, J.; Lang, B.; Nibbering, E. T. J.; Vauthey, E. *Angew. Chem., Int. Ed.* **2008**, *47*, 9044.
(21) Nibbering, E. T. J.; Fidder, H.; Pines, E. *Annu. Rev. Phys. Chem.* **2005**, *56*, 337.
(22) Doorley, G. W.; Wojdyla, M.; Watson, G. W.; Towrie, M.; Parker, A. W.; Kelly, J. M.; Quinn, S. J. *J. Phys. Chem. Lett.* **2013**, 2739.
(23) Swinnen, A. M.; Van der Auweraer, M.; de Schryver, F. C.; Makatani, K.; Okada, T.; Mataga, M. *J. Am. Chem. Soc.* **1987**, *109*, 321.
(24) Wasielewski, M. R.; Minsek, D. V.; Niemczyk, M. P.; Svec, W. A.; Yang, N. *J. Am. Chem. Soc.* **1990**, *112*, 2823.
(25) Banerji, N.; Angulo, G.; Barabanov, I. I.; Vauthey, E. *J. Phys. Chem. A* **2008**, *112*, 9665.
(26) Al Subi, A. H. A.; Niemi, M. M.; Tkachenko, N. V. N.; Lemmetyinen, H. H. *J. Phys. Chem. A* **2012**, *116*, 9653.
(27) Knibbe, H.; Rehm, D.; Weller, A. *Z. Phys. Chem.* **1967**, *56*, 95.
(28) Gould, I. R.; Young, R. H.; Mueller, L. J.; Farid, S. *J. Am. Chem. Soc.* **1994**, *116*, 8176.
(29) Iwai, S.; Murata, S.; Katoh, R.; Tachiya, M.; Kikuchi, K.; Takahashi, Y. *J. Chem. Phys.* **2000**, *112*, 7111.
(30) Kuzmin, M. G. M.; Soboleva, I. V. I; Dolotova, E. V. E.; Dogadkin, D. N. D. *Photochem. Photobiol. Sci.* **2003**, *2*, 967.
(31) Morandeira, A.; Fürstenberg, A.; Vauthey, E. *J. Phys. Chem. A* **2004**, *108*, 8190.
(32) Morteani, A. C. A.; Sreearunothai, P. P.; Herz, L. M. L.; Friend, R. H. R.; Silva, C. C. *Phys. Rev. Lett.* **2004**, *92*, 247402.
(33) Offermans, T.; van Hal, P. A.; Meskers, S. S.; Koetse, M. S.; Janssen, R. R. *Phys. Rev. B* **2005**, *72*, 045213 .
(34) Yin, C. C.; Kietzke, T. T.; Neher, D. D.; Hoerhold, H. H.-H. *Appl. Phys. Lett.* **2007**, *90*, 092117.
(35) Benson Smith, J. J.; Wilson, J. J.; Dyer Smith, C. C.; Mouri, K. K.; Yamaguchi, S. S.; Murata, H. H.; Nelson, J. J. *J. Phys. Chem. B* **2009**, *113*, 7794.
(36) Dyer Smith, C. C.; Benson Smith, J. J.; Murata, H. H.; Mitchell, W. J. W. *J. Phys. Chem. C* **2009**, *113*, 14533.
(37) Shepherd, W. E. B.; Platt, A. D. A.; Kendrick, M. J. M.; Loth, M. A. M.; Anthony, J. E. J.; Ostroverkhova, O. O. *J. Phys. Chem. Lett.* **2011**, *2*, 362.
(38) Stewart, D. J. D.; Dalton, M. J. M.; Swiger, R. N. R.; Cooper, T. M. T.; Haley, J. E. J.; Tan, L. L.-S. *J. Phys. Chem. A* **2013**, *117*, 3909.
(39) Chao, C. I.; Chen, S. A. *Appl. Phys. Lett.* **1998**, *73*, 426.
(40) Feng, J.; Li, F.; Gao, W. B.; Liu, S. Y.; Liu, Y. *Appl. Phys. Lett.* **2001**, *78*, 3947.
(41) D'Andrade, B. W.; Brooks, J.; Adamovich, V.; Thompson, M. E.; Forrest, S. R. *Adv. Mater.* **2002**, *14*, 1032.
(42) Morteani, A. C.; Friend, R. H.; Silva, C. *Chem. Phys. Lett.* **2004**, *391*, 81.
(43) Kim, J.-S.; Lu, L.; Sreearunothai, P.; Seeley, A.; Yim, K.-H.; Petrozza, A.; Murphy, C. E.; Beljonne, D.; Cornil, J.; Friend, R. H. *J. Am. Chem. Soc.* **2008**, *130*, 13120.
(44) Goushi, K.; Yoshida, K.; Sato, K.; Adachi, C. *Nat. Photonics* **2012**, *6*, 253.
(45) Crespo-Hernandez, C. E.; Cohen, B.; Hare, P. M.; Kohler, B. *Chem. Rev.* **2004**, *104*, 1977.
(46) Markovitsi, D.; Talbot, F.; Gustavsson, T.; Onidas, D.; Lazzarotto, E.; Marguet, S. *Nature* **2006**, *441*, E7.
(47) Takaya, T.; Su, C.; de La Harpe, K.; Crespo-Hernández, C. E.; Kohler, B. *Proc. Natl. Acad. Sci. U.S.A.* **2008**, *105*, 10285.
(48) Romero, E. E.; Diner, B. A. B.; Nixon, P. J. P.; Coleman, W. J. W.; Dekker, J. P. J.; van Grondelle, R. R. *Biophys. J.* **2012**, *103*, 185.
(49) Turro, N. J.; Ramamurthy, V.; Scaiano, J. C. *Modern molecular photochemistry of organic molecules*; University Science Books: Herndon, VA, 2010.
(50) Yang, N. C.; Libman, J. *J. Am. Chem. Soc.* **1973**, *95*, 5783.
(51) Mattes, S. L.; Farid, S. *Acc. Chem. Res.* **1982**, *15*, 80.
(52) Hui, M.-H.; Ware, W. R. *J. Am. Chem. Soc.* **1976**, *98*, 4718.
(53) Van Haver, P.; Helsen, N.; Depaemelaere, S.; Van der Auweraer, M.; De Schryver, F. C. *J. Am. Chem. Soc.* **1991**, *113*, 6849.
(54) Kikuchi, K. *J. Photochem. Photobiol. A* **1992**, *65*, 149.
(55) Kuzmin, M. G. *J. Photochem. Photobiol. A* **1996**, *102*, 51.
(56) Masuhara, H.; Mataga, N. *Acc. Chem. Res.* **1981**, *14*, 312.
(57) Mataga, N.; Kanda, Y.; Hirata, Y. *J. Phys. Chem.* **1983**, *87*, 1659.
(58) Huang, Y.-s.; Westenhoff, S.; Avilov, I.; Sreearunothai, P.; Hodgkiss, J. M.; Deleener, C.; Friend, R. H.; Beljonne, D. *Nat. Mater.* **2008**, *7*, 483.
(59) Bullock, J. E.; Carmieli, R.; Mickley, S. M.; Vura-Weis, J.; Wasielewski, M. R. *J. Am. Chem. Soc.* **2009**, *131*, 11919.
(60) Wasielewski, M. R. M. *Acc. Chem. Res.* **2009**, *42*, 1910.
(61) Heeger, A. J. A. *Chem. Soc. Rev.* **2010**, *39*, 2354.
(62) Bhosale, R.; Misek, J.; Sakai, N.; Matile, S. *Chem. Soc. Rev.* **2010**, *39*, 138.
(63) Dimitrov, S. D.; Bakulin, A. A.; Nielsen, C. B.; Schroeder, B. C.; Du, J.; Bronstein, H.; McCulloch, I.; Friend, R. H.; Durrant, J. R. *J. Am. Chem. Soc.* **2012**, *134*, 18189.
(64) Muller, P.-A.; Högemann, C.; Allonas, X.; Jacques, P.; Vauthey, E. *Chem. Phys. Lett.* **2000**, *326*, 321.
(65) Kattnig, D. R.; Rosspeintner, A.; Grampp, G. *Phys. Chem. Chem. Phys.* **2011**, *13*, 3446.
(66) Richert, S.; Rosspeintner, A.; Landgraf, S.; Grampp, G.; Vauthey, E.; Kattnig, D. R. *J. Am. Chem. Soc.* **2013**, *135*, 15144.
(67) Ottolenghi, M. *Acc. Chem. Res.* **1973**, *6*, 153.
(68) Vauthey, E.; Högemann, C.; Allonas, X. *J. Phys. Chem. A* **1998**, *102*, 7362.
(69) Kwok, W.-M.; Ma, C.; Phillips, D. L. *J. Phys. Chem. B* **2009**, *113*, 11527.
(70) Riddick, J. A.; Bunger, W. B. *Organic Solvents*; J. Wiley: New York, 1970.
(71) Weller, A. *Z. Phys. Chem.* **1982**, *133*, 93.
(72) Peover, M. E. *Trans. Faraday Soc.* **1962**, *58*, 2370.
(73) Vauthey, E. *J. Phys. Chem. A* **2001**, *105*, 340.
(74) Kikuchi, K.; Sato, C.; Watabe, M.; Ikeda, H.; Takahashi, Y.; Miyashi, T. *J. Am. Chem. Soc.* **1993**, *115*, 5180.
(75) Koch, M.; Rosspeintner, A.; Adamczyk, K.; Lang, B.; Dreyer, J.; Nibbering, E. T. J.; Vauthey, E. *J. Am. Chem. Soc.* **2013**, *135*, 9843.
(76) Murata, S.; Nishimura, M.; Matsuzaki, S. Y.; Tachiya, M. *Chem. Phys. Lett.* **1994**, *200*, 219.
(77) Angulo, G.; Kattnig, D. R.; Rosspeintner, A.; Grampp, G.; Vauthey, E. *Chem.—Eur. J.* **2010**, *16*, 2291.
(78) Rosspeintner, A.; Koch, M.; Angulo, G.; Vauthey, E. *J. Am. Chem. Soc.* **2012**, *134*, 11396.
(79) Birks, J. B.; Dyson, D. J. *Proc. R. Soc.* **1963**, *A275*, 135.
(80) Ware, W. R.; Richter, H. P. *J. Chem. Phys.* **1968**, *48*, 1595.
(81) Shida, T. *Electronic Absorption Spectra of Radical Ions*; Elsevier: Amsterdam, 1988; Vol. *34*, Physical Sciences data.
(82) Mohammed, O. F.; Vauthey, E. *J. Phys. Chem. A* **2008**, *112*, 5804.
(83) Pagès, S.; Lang, B.; Vauthey, E. *J. Phys. Chem. A* **2004**, *108*, 549.
(84) Haselbach, E.; Jacques, P.; Pilloud, D.; Suppan, P.; Vauthey, E. *J. Phys. Chem.* **1991**, *95*, 7115.

(85) Gladkikh, V.; Burshtein, A. I.; Angulo, G.; Pagès, S.; Lang, B.; Vauthey, E. *J. Phys. Chem. A* **2004**, *108*, 6667.
(86) Rosspeintner, A.; Kattnig, D. R.; Angulo, G.; Landgraf, S.; Grampp, G.; Cuetos, A. *Chem.—Eur. J.* **2007**, *13*, 6474.
(87) Burshtein, A. I. *Adv. Chem. Phys.* **2004**, *129*, 105.
(88) Arnold, B. R.; Farid, S.; Goodman, J. L.; Gould, I. R. *J. Am. Chem. Soc.* **1996**, *118*, 5482.
(89) Mataga, N.; Asahi, T.; Kanda, Y.; Okada, T.; Kakitani, T. *Chem. Phys.* **1988**, *127*, 249.
(90) Gould, I. R.; Ege, D.; Mattes, S. L.; Farid, S. *J. Am. Chem. Soc.* **1987**, *109*, 3794.
(91) Fleming, G. R. *Chemical Applications of Ultrafast Spectroscopy*; Oxford University Press: New York, 1986.
(92) Rubtsov, I. V.; Redmore, N. P.; Hochstrasser, R. M.; Therien, M. J. *J. Am. Chem. Soc.* **2004**, *126*, 2684.

NOTE ADDED AFTER ASAP PUBLICATION

A typographical error in equation 2 has been corrected in the version originally published February 26, 2014. The revised version was re-posted on March 3, 2014.